check for
updates

A MATHEMATICAL MODEL FOR DEHYDRATION BY SUCCESSIVE PRESSURE DROPS: SIMULATION OF DISCARDED POTATOES DEHYDRATION

Sebastian Gutierrez-Pacheco[1+]

Joahnn H. Palacios[2]

Alfonso Parra-Coronado[3]

Stéphane Godbout[4]

[1]*Ph.D. Candidate in Ecological Engineering, Faculty of Agriculture and Food Sciences, Laval University, Quebec, Canada.*
Email: sebastian.gutierrez-pacheco.1@ulaval.ca Tel: +14186562131
[2]*Research Assistant, Research and Development Institute for the Agri-Environment (IRDA), Quebec City, Canada.*
Email: joahnn.palacios@irda.qc.ca Tel: +14186432380 ext.606
[3]*Professor, Department of Civil and Agricultural Engineering, Universidad Nacional de Colombia, Bogota, Colombia.*
Email: aparrac@unal.edu.co Tel: +5713165000
[4]*Researcher, Research and Development Institute for the Agri-environment (IRDA), Quebec City, Canada.*
Email: stephane.godbout@irda.qc.ca Tel: +14186432380 ext.600

(+ Corresponding author)

ABSTRACT

Dehydration by Successive Pressure Drops (SPD) is a process with high potential for treating heat-sensitive materials; this includes agro-industry by-products. However, the response of drying kinetics to operating conditions of SPD is not fully understood. The present manuscript refers to mathematical simulations to describe drying kinetics of discarded potatoes using SPD. While there are numerous theoretical, semi-theorical and empirical mathematical models, the selection of the appropriate model is a rigorous process. In this paper, the Thompson thin-layer semi-theoretical model was chosen since the assumptions for this model (e.g., product is arranged in thin layers) are fulfilled for the SPD. As a result of mathematical simulation, it was possible to describe the drying kinetics in terms of the major parameters of SPD namely pressurizing level (Pa) and the Frequency of Pressure Drop (FPD). The dehydration by SPD allows the removal of water from the material, mainly at the pressure drop. If this stage occurs more frequently, the drying rate increases. The model developed describes at less 91% of the variability of the experimental data. It is recommended to use high FPD and Pa equals to 0.50 MPa.

Contribution/Originality: This study is one of the few studies explaining the application of a thin-layer model for Successive Pressure Drops drying of agro-industry by-products. This study originates new formula for drying kinetics of discarded potatoes based on the major parameters of Successive Pressure Drops drying namely pressurizing level and pressure drop frequency.

1. INTRODUCTION

The proportion of by-products, residues, and non-standard products generated by the agro-industry is a global predicament, from field production to commercialization (Galanakis, 2012). Evidence suggests that vegetable residues cause environmental pollution but also, they are an untreated source of biocomponents (Ajila, Brar, Verma, & Prasada Rao, 2012; FAOSTAT, 2020). Consequently, residue management systems are a key in the agricultural and agri-food sector due to the pressure exerted on both environment and natural resources protection, and sustainable development.

Animal and human food as well as extraction of biocomposites are reported as modern and sustainable procedures to use agri-food residues (Esteban, Garcia, Ramos, & Marquez, 2007). However, an effective conditioning of the material is generally compulsory due to a high moisture content (higher than 0.80 g g⁻¹ wet matter, Ajila et al. (2012) of agri-food residues. Consequently, they are highly biodegradable and both, hard and expensive to handle (Sotiropoulos, Malamis, Michailidis, Krokida, & Loizidou, 2016).

Several studies have focused on the use of hot air drying to reduce the moisture content of residues (Benseddik et al., 2020; Henríquez, Córdova, Almonacid, & Saavedra, 2014; Obied, Bedgood Jr, Prenzler, & Robards, 2008; Shah, Jani, & Khan, 2014; Wuttipalakorn, Srichumpuang, & Chiewchan, 2009). However, this technique is not adequate for some heat-sensitive agri-food by-products, as, the increase of the drying temperature results in an enzymatic and non-enzymatic degradation or decomposition of thermosensitive compounds (Gan, Ong, Chin, & Law, 2017; Larrauri, Rupérez, & Saura-Calixto, 1997; Mounir, Besombes, Al-Bitar, & Allaf, 2011). Thus, it is necessary to study the appropriate drying techniques to facilitate the management and conservation of this type of biomasses.

Dehydration by Successive Pressure Drops (SPD) is a process with high potential for treating heat-sensitive materials (Alonzo-Macías, Montejano-Gaitán, & Allaf, 2014; Bouallegue et al., 2020; Iguedjtal, Louka, & Allaf, 2008; Louati, Bahloul, Besombes, Allaf, & Kechaou, 2019; Louka & Allaf, 2004; Louka., Juhel, & Allaf, 2004). The operating principle in this process is to submit the material to successive changes between two pressure values Figure 1: a high-pressure level (P_a, with values up to 1 MPa) and a base pressure level (P_b or low pressure with values equal or lower than atmospheric pressure). These pressure levels are set for a respective period t_a and t_b, known as pressurizing phase and base pressure phase duration, respectively. Generally, the value of this period ranges from 5 to 35 seconds. These values cause the frequency of pressure drops (FPD) to vary between 0.50 to 12 depressions per minute. With this pressure changes, it is possible to (a) change the porosity of the material, which improves the drying kinetics, (b) create an instantaneous airflow which removes the water from the surface of the material, and, (c) when the vacuum is established, reduce the evaporation temperature of the water contained in the material (Mounir, Téllez-Pérez, Alonzo-Macías, & Allaf, 2014).
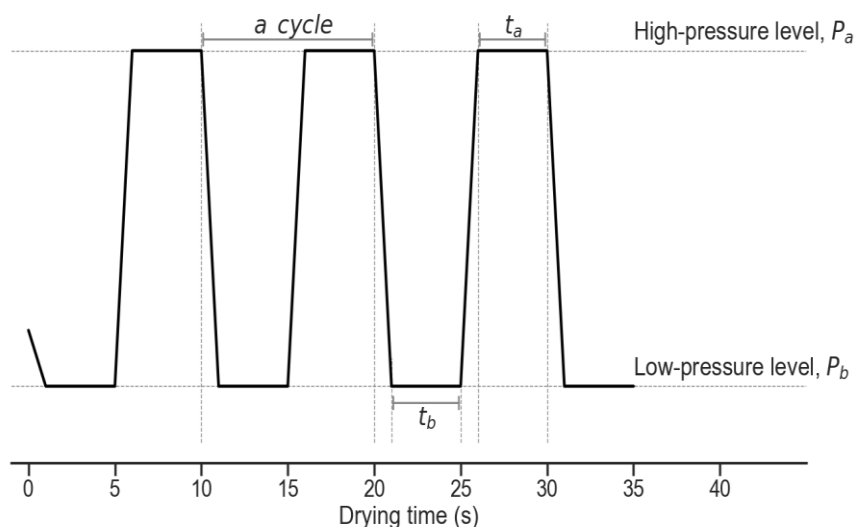

Figure-1. Pressure variations in dehydration by Successive Pressure Drops (SPD).

To make recommendations about sizing and operation of a dehydrator by SPD for agri-food residues, two ways are established: to conduct experimental studies, being an expensive procedure (Chou, Chua, Teoh, & Ho, 2006; Haddad, Juhel, Louka, & Allaf, 2004; Louati et al., 2019; Maache-Rezzoug, Rezzoug, & Allaf, 2001; Maache-Rezzoug, Rezzoug, & Allaf, 2002; Parra-Coronado, Roa-Mejía, & Oliveros-Tascón, 2008; Rakotozafy, Louka, Therisod, Thérisod, & Allaf, 2000), and to develop a mathematical simulation of drying assisted by computer (Al

Haddad, 2007; Henríquez et al., 2014; Kaveh & Amiri Chayjan, 2017; Parra-Coronado, 1993; Roa et al., 1999; Sadeghi, Movagharnejad, & Haghighi Asl, 2019; Thompson, Peart, & Foster, 1968).

Mathematical simulation is a practical tool to design an appropriate implementation of new dryers. The simulation of various drying systems involves solving a set of heat and mass-transfer equations, which describe (a) heat and moisture exchange between product and air, (b) psychrometric properties of moist air, (c) adsorption and desorption rates of heat and moisture transfer, and (d) equilibrium relations between product and air (Ertekin & Firat, 2017). The heat is required to evaporate the moisture, which is removed from the drying product surface by the external drying medium, usually air. Generally, the moist agri-food by-products dry in constant rate, followed by a subsequent period where drying rate is lower, and it stops when an equilibrium is established. There are theoretical, semi-theoretical and empirical relationships to predict the drying behaviour of different products in those periods. Theoretical models (generally based on Fick's second law of diffusion) are rigorous and difficult to apply because of the large number of unknown parameters (Erbay & Icier, 2010). Those models consider both the internal and external heat and mass transfer, and predict better the temperature and the moisture gradient in the product. However, simpler options have been applied instead. The characteristic drying curves (Fyhr & Kemp, 1998) obtained from thin-layer drying equations are the most used models for predicting the drying rate. They are easier and need fewer assumptions due to the use of some experimental data. The models are then used to predict drying rates at conditions different from the reference case, and even changing some parameters associated with the dehydrator.

For this last category, one of the most popular mathematical models for static bed dryers is the Thompson thin-layer model (Kaveh & Amiri Chayjan, 2017; Thompson et al., 1968). It is a semi-theoretical model, originally developed to simulate grains corn drying. In this model, the thick layer of corn kernels is divided into many thin layers (thickness around one inch), placed one over the other. Then drying is calculated as a heat and mass balance in each of the different layers, integrating them at the simulation process end. This semi-theoretical model has proved useful for the dryer designers (Brooker, Bakker Arkema, & Hall, 1974). This model can generate errors in the estimations by assuming a uniform product temperature (in some cases, equivalent of the room temperature) at the beginning of the simulation. However, this error occurs only at the beginning of the process and it may be reduced to acceptable values with reducing the thickness of the product (Erbay & Icier, 2010; Henderson & Pabis, 1961).

Because the product is arranged in thin layers into the treatment chamber of SPD dehydrator, one on top of the other, the Thompson thin-layer model can be used to simulate the kinetics of drying as a function of pressurization times (t_a and t_b) and pressure levels (P_a and P_b). The aim of this work is to simulate the operating conditions of the SPD dehydrator and to define the configuration that allows the best drying kinetics for the drying of discarded potatoes due to poor quality. To achieve this goal, the study aimed 1) to develop a model adapted to the SPD, 2) to calibrate the best-performed single-thin-layer equation according to the SPD operation parameters, and 3) to validate model reliability using values obtained from experimental trials.

2. DEVELOPMENT OF THE MATHEMATICAL SIMULATION

The implementation of the Thompson thin-layer model represents the passage of air initially at a temperature (T) and a humidity ratio (H), through the first thin layer of product that has an initial moisture content (M) and a temperature (θ). The air outflow conditions of the first thin layer of product are the entrance conditions for the next layer, and so on until the thick layer of product is completed. After an interval of time, a certain amount of moisture evaporates, being removed by the air because of pressure drops. The model estimated the evolution of the moisture content along drying time, under the predetermined operating conditions. To adjust a thin-layer drying equation, the SPD was represented as a tray dryer with the same airflow generated by the sudden pressure drop. Therefore, it

was assumed that the removal of water occurs only during the pressure drop lapse (when pressure changed from P_a to P_b, Figure 1).

2.1. Airflow Estimation

The sudden pressure drops in the SPD dehydrator results in the instantaneous release of an air mass (increasing kinetic energy), producing an instant convection and moisture reduction of the material. Airflow (q in m^3 min^{-1}) was calculated by Equation 1 (Gutierrez-Pacheco, 2016).

$$q = \left(\frac{\Delta P \cdot d^5 \cdot P_a}{75.7 \cdot L}\right)^{\frac{1}{1.85}} \cdot t_{drop} \cdot FPD \tag{1}$$

Where ΔP represents the pressure drop (kg cm^{-2}), d is the pipe/air outlet valve diameter (mm), P_a is the pressurizing level (kg cm^{-2}), L is the length of the pipe/outlet valve (mm), t_{drop} is the pressure drop duration (approximately 1/60 min), FPD is the frequency of pressure drops (drops min^{-1}), and 75.7 is the conversion factor to obtain the air flow in m^3 min^{-1}.

2.2. Calculation of the Product-Air Amount Ratio (R)

The R factor was necessary to make the equivalence between the water lost by the product and transferred to the air. The calculated difference in moisture of the product for each iteration is multiplied by this factor and added to the humidity ratio of the drying air. The R factor was determined by Equation 2 (Gutierrez-Pacheco, 2016).

$$R = \frac{v_{air} \cdot adm}{q \cdot \Delta t} \tag{2}$$

Where R is the product-air amount ratio (kg of product kg^{-1} of air), v_{air} is the specific volume of air (m^3 kg^{-1}), q is the airflow (m^3 h^{-1}) generated by each cycle of pressure drop, Δt is the time interval adopted for each iteration (one hour), and adm is the amount of dry matter in the treatment chamber (kg of dry product).

2.3. Heat Balance before Drying

For each time interval (Δt), the Thompson model (Kaveh & Amiri Chayjan, 2017; Thompson et al., 1968) determined the equilibrium temperature (T_e) between the drying air and the product. This sensible heat balance was represented by Equation 3. Where H is the air humidity ratio (kg of water kg^{-1} of dry air), T is the air temperature (°C), C_p is the specific heat of the product (kJ kg^{-1} °C^{-1}), and θ is the product temperature (°C).

$$T_e = \frac{(1.0048 + 1.88 \cdot H) \cdot T + C_p \cdot \theta}{1.0048 + 1.88 \cdot H + C_p} \tag{3}$$

2.4. Heat Balance after Drying

The Thompson model also allows a post-drying heat balance to determinate the air and the dried product temperature (T_f) after the time interval (Δt). It is assumed that the moisture lost by the product (ΔM) is removed by air, which increases its humidity ratio to H_f. Equation 4 allows this calculation.

$$T_f = \frac{(1.0048 + 1.88 \cdot H_0) \cdot T_e - \Delta M \cdot (2461.42 + LHV - T_e) + (C_p \cdot T_e)}{1.0048 + 1.88 \cdot H_f + C_p} \tag{4}$$

Where H is the air humidity ratio (kg of water kg^{-1} of dry air), and the subscript o and f represent the initial and final values for each iteration, respectively, T_e is the equilibrium temperature (Equation 3, °C), LHV is the

latent heat of vaporization (Equation 6, kJ kg^{-1}), and C$_p$ is the specific heat of the product (kJ kg^{-1} °C^{-1}).

Other additional parameters were considered: Expected final moisture content (wet matter) of 10% and specific heat (C$_p$) of 3,603 kJ kg^{-1} °C^{-1} (Araya-Farias & Ratti, 2009). For the purposes of this publication, the specific heat of the product (C$_p$) was considered as a constant (invariable against changes in humidity).

The bulk density (ρ_p, in kg m^{-3}) and latent heat of vaporization (LHV, in kJ kg^{-1}) of the product were recalculated for each iteration according to Equation 5 (Key-Technology, 2015) and 6 (Chen, 2006) respectively.

$$\rho_p = 305 + 5.89 \cdot M_i \cdot 100 \qquad (5)$$

$$LVH = 1512.9 \cdot (M_i \cdot 100)^{-9.744} + 0.461 \cdot \left(6887 - 5.31 \cdot (\theta + 273.15)\right) \quad (6)$$

Where M$_i$ is the moisture content of the product (g g^{-1} dry matter, d.m.) and θ is the product temperature (°C) for each iteration.

2.5. Thin-Layer Drying Equation

Finally, this mathematical model required a single-thin-layer equation (Equation 7) calibrated for the SPD conditions to be analyzed. This equation had to be a function of the product's moisture content (M), time (t) and the most relevant parameters of the SPD (e.g. frequency of pressure drops, FPD, and pressure levels, P$_a$ and P$_b$). This equation incorporated all transport properties in function of the drying mechanism. For SPD drying technique, a thin layer equation has not been developed, so the first step was to determine the equation describing the drying kinetics by SPD. The procedure for selecting this equation is described in the materials and methods section.

$$\frac{dM}{dt} = f(M, P_a, P_b, FPD, ..., t) \qquad (7)$$

3. MATERIALS AND METHODS

3.1. Dehydrator Prototype and Operation Description

Figure 2 describes the SPD dehydrator set up. Each test started with compressor activation (Figure 2, B). P$_a$ was established using a pressure regulator (Figure 2, D). The first cycle began with the opening of the valve F, to establish the P$_b$ level in the treatment chamber (Figure 2, G) (in this case, P$_b$ equals to atmospheric pressure, P$_{atm}$). Then, valve F remained closed during the base pressure phase (t$_b$) and then, the valve D was open to pressurize the treatment chamber. Finally, the valves D and F were closed during the pressurizing phase (t$_a$). Subsequently, the cycle was repeated until test duration was reached.
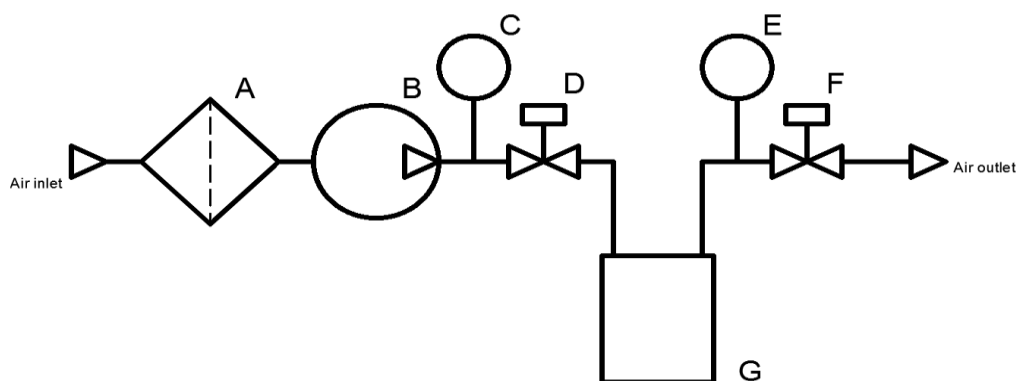

Figure-2. SPD set up diagram. A) air filter, B) compressor and compressed air tank, C and E) pressure gauges, D and F) solenoid valves compressor, G) treatment chamber.

3.2. Raw Material and Experimental Data

Discarded potatoes (cultivar Russet Burbank) for the presence of sprouts were used as raw material. For each test, samples of 30 g were cut into rectangular prisms 20 mm x 10 mm x 5 mm and placed in the SPD device. The weight of the samples was recorded every 30 minutes to determine the variation of moisture content during drying. Samples were weighted using an electronic scale (Mettler PM2000 precision 0.1 g - Columbus, OH, USA). To determine the dry weight, at the end of each treatment, each sample was dehydrated in the oven (Carbolite LHT 6/120 - Hope Valley, UK) for 24 hours at 60 °C. Moisture content was calculated by Equation 8:

$$M_i = \frac{W_i - W_{dry}}{W_{dry}} \qquad (8)$$

M_i is the moisture content (g g⁻¹ dry matter, d.m.) for drying time i, W_i is the weight of the wet sample (g) and W_{dry} is the weight of the dry sample (g).

For model calibration and validation, four SPD configurations were performed, summarized in Table 1. Each test had a duration of six hours. Four repetitions were made for each configuration, three repetitions for the calibration of the model and one for validation of model reliability.

Table-1. Summary of experimental configurations for model validation.

Treatment*	Pressurizing level, P_a (gauge pressure in MPa)	Frequency of pressure drops, *FPD* (number of depressions per minute)
DSPD 1	0.30	6
DSPD 2	0.30	12
DSPD 3	0.50	12
DSPD 4	0.60	12

Note: *Each treatment had four repetitions. Three for the calibration of the single-thin-layer equations and one for the validation of the model.

3.3. Thin-Layer Drying Equation

Three repetitions for each treatment Table 1 were used for the calibration of the single-thin-layer equation Equation 7. Since no calibrated thin layer equation has been reported for SPD, the first step was to determine the equation describing the drying kinetics by SPD. The experimental moisture content values versus the drying time were fitted using four common thin-layer equations used to explain the drying kinetics of foods Table 2. The empirical constants for the models were obtained using Microsoft office Excel Solver.

Table-2. Thin-layer equations tested to describe dehydration of potatoes by SPD.

Model name	Equation*	Reference
Newton	$M_i = M_0 * e^{-\kappa t}$	Lewis (1921)
Henderson-Pabis	$M_i = M_0 * \alpha * e^{-\kappa t}$	Henderson and Pabis (1961)
Logarithmic	$M_i = M_0(\alpha * e^{-\kappa t} + \gamma)$	Yagcioglu, Degirmencioglu, and Cagatay (1999)
Wang-Singh	$M_i = M_0(\alpha * t^2 + \beta * t + 1)$	Wang and Singh (1978)

Note: *M_i is the moisture content (kg kg⁻¹ dry matter) for each time i, M_0 is the initial moisture content (kg kg⁻¹ dry matter), t is the drying time (hours), α, β, γ and κ are empirical constants.

Newton's equation represents a simple exponential of the drying kinetics as a first-order model. Henderson-Pabis equation presents an additional parameter that can improve the fitting, but if the estimated value of the parameter α is different from 1, the moisture content will not assume a value equal to M_0 at the initial time, which invalidates the mathematical consistence of model. Logarithmic equation is mathematically consistent at the initial time only if the estimated values of parameters α and γ present a sum equal to 1. Finally, Wang-Singh equation is a second order empirical model, consistent for the initial moisture content value. Lastly, the shrinkage phenomenon

was assumed as negligible, although it is widely well known that it is notorious in fruit dehydration (Chemkhi & Zagrouba, 2011; Frias, Clemente, & Mulet, 2010; Mounir et al., 2014).

The best-performance equation in the calibration will be chosen. This equation will be adjusted to obtain the drying kinetics of a thin layer according to the operating conditions of the SPD.

3.4. Performance Criteria

Mathematical simulations were computer-assisted and were implemented in Microsoft Visual Basic programming language for applications 7.0. The drying kinetics calculated the conditions of the drying air (temperature, T, and humidity ratio, H) and the conditions of the product (moisture content, M, and temperature, θ). It was an iterative process for the four layers of product disposed in the SPD, and time step between each simulation was one hour. These simulated values were compared with the values observed in the experimental samples (one sample per treatment).

To quantify the accuracy of estimation, three statistical evaluation criteria were used. Coefficient of determination (R^2, Equation 9), the root-mean-square error (RMSE, Equation 10), and the Nash-Sutcliffe Coefficient (NS, Equation 11). These criteria described the statistical correlation between the estimated and observed data.

The coefficient of determination (R^2):

$$R^2 = 1 - \frac{\sum_{i=1}^{N}\left(Y_{exp,i}-Y_{sim,i}\right)^2}{\sum_{i=1}^{N}Y_{exp,i}^2-\frac{\sum_{i=1}^{N}Y_{sim,i}^2}{N}} \tag{9}$$

The root-mean square error (RMSE):

$$RMSE = \sqrt{\frac{\sum_{i=1}^{N}\left(Y_{exp,i}-Y_{sim,i}\right)^2}{N}} \tag{10}$$

And the Nash-Sutcliffe Coefficient (NS):

$$NS = \frac{\sum_{i=1}^{N}\left(Y_{exp,i}-Y_{sim,i}\right)^2}{\sum_{i=1}^{N}\left(Y_{exp,i}-\bar{Y}_{exp}\right)^2} \tag{11}$$

Where Y is the moisture content for each iteration (dry matter), the subscripts *exp* and *sim* refer to the experimental and simulated values, respectively, $\bar{Y}$ is the mean of observed moisture content, and N the number of observations. The best fit is achieved when the RMSE is close to zero, and both, NS and R^2 are close to one. In this study, RMSE and NS statistics were used to measure the model performance for forecasting product moisture content whereas R^2 was used to analyze the linear regression goodness of fit between observed and estimated data. Also, for model goodness of fit, the intercept and gradient should be close to zero and one, respectively.

4. RESULTS AND DISCUSSION

4.1. Calibration of Single-Thin-Layer Equation

The thin-layer equations studied Table 2 were adjusted for the experimental data of the different drying conditions Table 1. The estimated parameters for models are presented in Table 3. Also, calibration performance (RMSE, R^2 and NS coefficients) from each equation are presented in Table 4. According to the results, the calibration process is satisfactory (calculated coefficients of determination greater than 0.98). The RMSE values obtained from the adjustment procedure show the goodness of the calibration of the single-thin-layer models tested to describe the different SPD configurations. Calculated RMSE values were less than 0.07. However, despite the Logarithmic and the Wang and Singh models have a good fit (low RMSE value and NS and R^2 values close to one, Table 4, predictions of negative moisture values were obtained, which is not coherent.

Table-3. Estimated parameters of the models examined to describe the drying kinetics of potato residues by SPD.

Treatments	Calculated air flow (m³ min⁻¹)	Model name							
		Newton		Henderson–Pabis		Logarithmic		Wang–Singh	
DSPD 1	4.34	κ	1.653[d]	α	1.071[a]	α	1.73[a]	α	0.2754[c]
				κ	1.755[d]	κ	0.7159[d]	β	-1.135[a]
						γ	-0.708[b]		
DSPD 2	8.68	κ	2.353[c]	α	1.046[ab]	α	1.172[b]	α	0.7167[b]
				κ	2.434[c]	κ	1.755[c]	β	-1.67[b]
						γ	-0.151[a]		
DSPD 3	14.23	κ	3.108[a]	α	1.027[b]	α	1.12[b]	α	1.039[a]
				κ	3.167[a]	κ	2.669[a]	β	-2.043[c]
						γ	-0.083[a]		
DSPD 4	17.08	κ	2.838[b]	α	1.041[ab]	α	1.074[b]	α	0.9398[a]
				κ	2.919[b]	κ	2.272[b]	β	-1.935[c]
						γ	-0.098[a]		

Note: DSPD: Dehydrator configuration by successive pressure drops. DSPD 1: P_a = 0.3 MPa, FDP = 6. DSPD 2: P_a = 0.3 MPa, FDP = 12. DSPD 3: P_a = 0.5 MPa, FDP = 12. DSPD 4: P_a = 0.6 MPa, FDP = 12.
Different superscripts between parameters of the same model represent statistical differences in mean values (p <0.05).

Newton's model was chosen due to its simplicity to describe the single-thin-layer drying as a function of the airflow (q) generated by the pressure drop. Significant differences between the values of the parameter κ were obtained. The parameter κ of this model can be expressed as a function of the estimated flow rate after the pressure drop, which is a function of the pressure difference ($P_a - P_b$) and the frequency of pressure drops (FPD). For this, Equation 12 was obtained.

$$\kappa = 3.6543 \cdot e^{\left(-\frac{3.473}{q}\right)} \tag{12}$$

Table-4. Performance criteria values thin-layer models examined to describe the drying kinetics of potato residues by SPD.

Treatments	Performance criteria	Model name			
		Newton	Henderson–Pabis	Logarithmic	Wang–Singh
DSPD 1	R^2	0.981	0.984	0.997	0.997
	RMSE	0.07	0.06	0.03	0.03
	NS	0.952	0.959	0.992	0.992
DSPD 2	R^2	0.985	0.987	0.993	0.996
	RMSE	0.05	0.05	0.03	0.03
	NS	0.973	0.977	0.988	0.993
DSPD 3	R^2	0.993	0.993	0.993	0.996
	RMSE	0.03	0.03	0.03	0.02
	NS	0.989	0.990	0.990	0.995
DSPD 4	R^2	0.983	0.984	0.992	0.997
	RMSE	0.05	0.05	0.03	0.02
	NS	0.974	0.976	0.988	0.996

Note: DSPD: Dehydrator configuration by successive pressure drops. DSPD 1: P_a = 0.3 MPa, FDP = 6. DSPD 2: P_a = 0.3 MPa, FDP = 12. DSPD 3: P_a = 0.5 MPa, FDP = 12. DSPD 4: P_a = 0.6 MPa, FDP = 12.

The pressure drop and pressure drop frequency are the variables to be controlled in the SPD. A comparison of the findings with those of other studies (Al Haddad, 2007; Chou et al., 2006; Maache-Rezzoug et al., 2001; Maache-Rezzoug. et al., 2002; Rakotozafy et al., 2000) confirms drying kinetics is explained by these two factors.

4.2. Effect of Pressure Drop Frequency

Frequency has a positive effect on drying kinetics. According to the parameter analysis, parameter κ of Newton model increased from 1.653 to 2.353 when the FPD changed from 6 to 12 pressure drops per minute. Greater number of depressions per minute generates greater volume of air passing through the drying chamber and allowing faster drying. This corresponds with results reported by Chou et al. (2006) for dried pork tissue, Chua and

Chou (2004) for potato and carrot, and by Rakotozafy et al. (2000) for baker's yeast. Figure 3 illustrates moisture content simulated for 6 and 12 pressure drops per minute (DSPD 1 and DSPD 2, respectively). The prediction of the data under the developed model varied 96 and 91%, respectively. The results for these two treatments describe that drying kinetics improves when *FPD* increases. However, prediction of final moisture content and drying time should be improved.
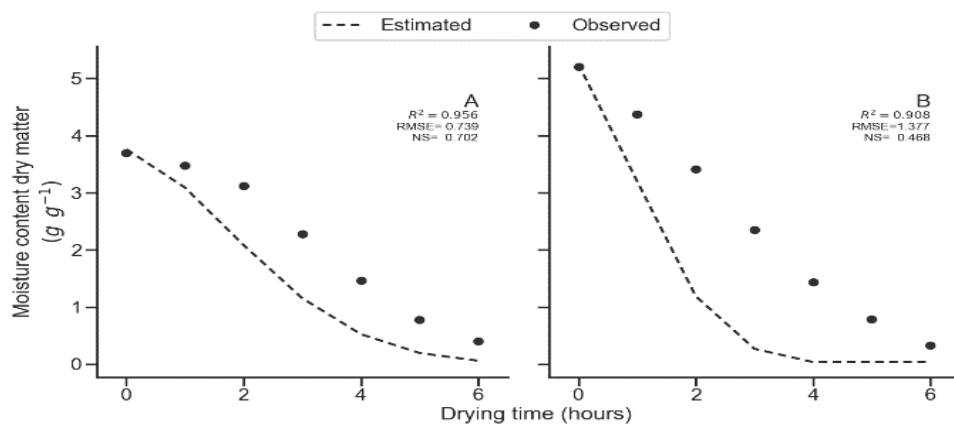

Figure-3. Drying curves for SPD configured for different pressure drop frequency. Comparison of experimental and simulated results. A: Treatment DSPD 1, 6 pressure drops per minute. B: Treatment DSPD 2, 12 pressure drops per minute.

Drying by SPD allows the removal of water from the material mainly during the pressure drop. At this stage, a certain amount of liquid water passes into vapor, from product to drying air, to restore partial vapor pressure (Cong, Haddad, Rezzoug, Lefevre, & Allaf, 2008). Therefore, if this stage occurs more frequently (higher *FPD*), the drying rate increases. The drying frequency can increase up to the limit of system response. In this case, by the response time of the solenoid valves. The highest frequency that can be achieved is 15 pressure drops per minute (cycle duration of 4 s).

4.3. Pressurizing Level Effect

The effect of pressure P_a can be analyzed with DSPD treatments 2, 3 and 4 (P_a = 0.3, 0.5 and 0.6 MPa, respectively). Figure 4 illustrates experimental and simulated results for each treatment. The prediction of drying kinetics for these treatments varied from 91 to 98%. The drying rate increased when P_a changed from 0.3 to 0.5 MPa. However, when high P_a values (0.5 and 0.6 MPa) were established, drying kinetics was similar. This coincides with Rakotozafy et al. (2000) who estimated a response surface for the yeast drying rate by SPD. Their results showed that the drying rate stabilizes for pressures greater than 0.46 MPa. This behaviour was represented by the developed simulation model.
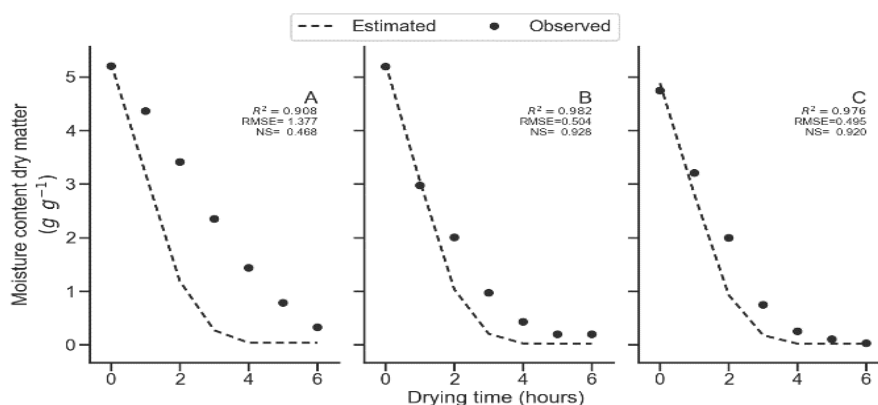

Figure-4. Drying curves for SPD configured for different pressurizing level. Comparison of experimental and simulated results. A: Treatment DSPD 2, P_a = 0.3 MPa; B: Treatment DSPD 3, P_a = 0.5 MPa; C: Treatment DSPD 4, P_a = 0.6 MPa.

The current study adopted atmospheric pressure as P_b. Previous studies (Alonzo-Macías et al., 2014; Cong et al., 2008; Louka & Allaf, 2004) that have settled P_b value below atmospheric pressure observed some advantages such as product texturization and high organoleptic quality. To set P_b below atmospheric pressure, the necessary vacuum equipment is required (vacuum pump and vacuum chamber up to 130 times larger than the drying chamber, Maache-Rezzoug. et al. (2002); Alonzo-Macías et al. (2014). So, if the goal is only to improve the drying kinetics, setting P_b equal to atmospheric pressure and P_a greater than 0.5 MPa is pertinent (Cong et al., 2008).

4.4. Model for Drying Kinetics of Discarded Potatoes

Considering Equation 1 to 7, Equation 7 being Newton's equation calibrated (κ parameter as a function of airflow, Equation 12), the validation process was satisfactory. Calculated coefficients of determination greater than 0.90, and calculated RMSE values were less than 1.4 Table 5.

Table-5. Performance criteria values (R² and RMSE), and final moisture values for the different SPD treatments.

	Treatments			
	DSPD 1	**DSPD 2**	**DSPD 3**	**DSPD 4**
R²	0.956	0.908	0.983	0.976
RMSE	0.74	1.38	0.50	0.50
Final moisture (g g⁻¹, d.m.)	0.40	0.33	0.20	0.03

Note: DSPD: Dehydrator configuration by successive pressure drops. DSPD 1: P_a = 0.3 MPa, *FDP* = 6. DSPD 2: P_a = 0.3 MPa, *FDP* = 12. DSPD 3: P_a = 0.5 MPa, *FDP* = 12. DSPD 4: P_a = 0.6 MPa, *FDP* = 12.

4.5. Validation

The selected thin-layer model is Newton's model and its parameter κ could be expressed as a function of the air flow Equation 12. This relation between κ and airflow was also reported by Yaldız (2001) and Hossain and Bala (2002). The κ value increases as the air flow increases, in consequence, the drying time decreases. However, there is a point at where the κ value starts to be constant. In this study, this is achieved when the pressurization level is 0.5 MPa. These results further support the idea of Rakotozafy et al. (2000) and Maache-Rezzoug et al. (2002) referring that an increase of pressurizing level above 0.5 MPa is not statistically significant for drying rate.

Newton's thin-layer model was integrated into Thompson's model, making the balance of energy and mass between the different layers. Thompson's model estimations are close to the observed drying curves. The developed model explains at least 91% of the drying of discarded potatoes through the SPD (Table 5). The fitting procedure indicated that the assumptions made to describe the SPD drying process are valid for discarded potatoes drying. These assumptions are: The airflow is a function of the pressure drop ($P_a - P_b$) and *FPD* Equation 12; every thin layer of product are subjected to the same air flow, therefore a ratio between the amount of air and the amount of product is established by Equation 5; and, the thin-layer drying equation is known and can be expressed as a function of the drying condition (in this case the level of pressurization, P_a).

The present SPD prototype has the air inlet and outlet on the top of the product. This can lead to non-uniform final moisture content and consequently problems in product storage. Further studies need to be carried out to evaluate the influence of this variable on drying kinetics and drying uniformity, and then, optimise the system if necessary.

5. CONCLUSIONS

The present research proposed a mathematical model for the operation conditions of the SPD system. About the objectives set out at the beginning of the manuscript:

1) This manuscript describes the model adapted for the SPD system. The kinetics of SPD drying is largely controlled by the pressure drop generated ($P_a - P_b$) and the frequency of pressure drops (*FPD*).

2) Four single-thin-layer equations were tested in model calibration stage. Newton's equation was chosen due to its simplicity to describe the single-thin-layer drying as a function of the airflow generated by the pressure drop.

3) At least 91% of the variation of experimental data was explained by the mathematical model implemented. The final thin-layer model for drying kinetics considered that a) each of the product thin-layers are subjected to the same amount of air, thus generating a product-air amount ratio; and, b) the single-thin-layer drying equation (Newton's equation) is known and can be expressed as a function of the SPD operation parameters (P_a, P_b and *FPD*).

To obtain the greatest drying speed, the following SPD configuration is recommended: a) Use atmospheric pressure as P_b, which avoids the use of equipment to generate vacuum, b) Establish high *FPD*, c) Set high pressurization value (P_a) to 0.5 MPa.

Further studies need to be carried out to evaluate the influence of air inlet and outlet position on drying kinetics and drying uniformity. Air circulation can lead to non-uniform final moisture content and at the same time can change the drying kinetics of the SPD.

REFERENCES

Ajila, C. M., Brar, S. K., Verma, M., & Prasada Rao, U. J. S. (2012). Sustainable solutions for agro processing waste management: An overview. In Environmental Protection Strategies for Sustainable Development (pp. 65–109). Netherlands: Springer.

Al Haddad, M. (2007). *Theoretical contribution and modeling of instantaneous phenomena in self-spraying and spraying operations dehydration*. Doctoral Dissertation HAL Archives-Ouvertes.fr (tel-00399138) University of La Rochelle, La Rochelle, France.

Alonzo-Macías, M., Montejano-Gaitán, G., & Allaf, K. (2014). Impact of drying processes on strawberry (Fragaria var. Camarosa) texture: Identification of crispy and crunchy features by instrumental measurement. *Journal of Texture Studies, 45*(3), 246–259. Available at: https://doi.org/10.1111/jtxs.12070.

Araya-Farias, M., & Ratti, C. (2009). Dehydration of foods: General concepts. In C. Ratti (Eds.), Advances in food dehydration (1st ed., pp. 1–36). Boca Raton, FL: CRC Press.

Benseddik, A., Azzi, A., Lalmi, D., Bensaha, H., Zidoune, M. N., & Allaf, K. (2020). Empirical mathematical model to evaluate the effective diffusivity of pumpkin slice during forced air convection dryer. In B. S. Belasri A. (Ed.), ICREEC 2019. Springer Proceedings in Energy (pp. 45–52). Singapore: Springer.

Bouallegue, K., Allaf, T., Younes, R. B., Téllez-Pérez, C., Besombes, C., & Allaf, K. (2020). Pressure, temperature and processing time in enhancing Camelina sativa oil extraction by Instant Controlled Pressure-Drop (DIC) texturing pre-treatment. *Grasas y Aceites, 71*(3), e365–e365. Available at: https://doi.org/10.3989/GYA.0337191365.

Brooker, D. B., Bakker Arkema, F. W., & Hall, C. W. (1974). *Drying cereal grains*. Madison, WI: AVI Publishing Company.

Chemkhi, S., & Zagrouba, F. (2011). Characterisation of potato slices during drying: Density, shrinkage, and thermodynamic of sorption. *International Journal of Food Engineering, 7*(3), 8. Available at: http://dx.doi.org/10.2202/1556-3758.2349.

Chen, C. (2006). Obtaining the isosteric sorption heat directly by sorption isotherm equations. *Journal of Food Engineering, 74*(2), 178–185. Available at: https://doi.org/10.1016/j.jfoodeng.2005.01.041.

Chou, S. K., Chua, K. J., Teoh, S. H., & Ho, J. C. (2006). Drying of porcine dermal tissue via pressure swing adsorption. *Drying Technology, 24*(8), 973–982. Available at: https://doi.org/10.1080/07373930600776126.

Chua, K., & Chou, S. (2004). On the experimental study of a pressure regulatory system for bioproducts dehydration. *Journal of Food Engineering, 62*(2), 151-158. Available at: https://doi.org/10.1016/S0260-8774(03)00226-7.

Cong, D. T., Haddad, M. A., Rezzoug, Z., Lefevre, L., & Allaf, K. (2008). Dehydration by successive pressure drops for drying paddy rice treated by instant controlled pressure drop. *Drying Technology, 26*(4), 443-451. Available at: https://doi.org/10.1080/07373930801929300.

Erbay, Z., & Icier, F. (2010). A review of thin layer drying of foods: Theory, modeling, and experimental results. *Critical Reviews in food Science and Nutrition, 50*(5), 441-464.

Ertekin, C., & Firat, M. Z. (2017). A comprehensive review of thin-layer drying models used in agricultural products. *Critical Reviews in Food Science and Nutrition, 57*(4), 701-717. Available at: https://doi.org/10.1080/10408398.2014.910493.

Esteban, M., Garcia, A., Ramos, P., & Marquez, M. (2007). Evaluation of fruit–vegetable and fish wastes as alternative feedstuffs in pig diets. *Waste Management, 27*(2), 193-200. Available at: https://doi.org/10.1016/j.wasman.2006.01.004.

FAOSTAT. (2020). Food balance sheets. Supply utilization accounts. Food and agriculture organization of the United Nations. Retrieved from http://www.fao.org/faostat/en/#data/SCL.

Frias, A., Clemente, G., & Mulet, A. (2010). Potato shrinkage during hot air drying. *Food Science and Technology International, 16*(4), 337-341. Available at: https://doi.org/10.1177/1082013210366967.

Fyhr, C., & Kemp, I. C. (1998). Comparison of different drying kinetics models for single particles. *Drying Technology, 16*(7), 1339-1369. Available at: https://doi.org/10.1080/07373939808917465.

Galanakis, C. M. (2012). Recovery of high added-value components from food wastes: Conventional, emerging technologies and commercialized applications. *Trends in Food Science & Technology, 26*(2), 68-87. Available at: https://doi.org/10.1016/j.tifs.2012.03.003.

Gan, S. H., Ong, S. P., Chin, N. L., & Law, C. L. (2017). Kinetic retention of sialic acid and antioxidants in Malaysian edible bird's nest during low-temperature drying. *Drying Technology, 35*(7), 827-837. Available at: https://doi.org/10.1080/07373937.2016.1219741.

Gutierrez-Pacheco, S. (2016). *Design, implementation and evaluation of a dehydration system due to cyclical pressure changes for agro-industrial waste.* Master's Thesis.

Haddad, J., Juhel, F., Louka, N., & Allaf, K. (2004). A study of dehydration of fish using successive pressure drops (DDS) and controlled instantaneous pressure drop (DIC). *Drying Technology, 22*(3), 457-478. Available at: https://doi.org/10.1081/DRT-120029993.

Henderson, S. M., & Pabis, S. (1961). Grain drying theory I. Temperature effect on drying coefficient. *Journal of Agricultural Engineering Research, 6*(3), 169–174.

Henríquez, C., Córdova, A., Almonacid, S., & Saavedra, J. (2014). Kinetic modeling of phenolic compound degradation during drum-drying of apple peel by-products. *Journal of Food Engineering, 143*, 146-153. Available at: https://doi.org/10.1016/j.jfoodeng.2014.06.037.

Hossain, M., & Bala, B. (2002). Thin-layer drying characteristics for green chilli. *Drying Technology, 20*(2), 489-505. Available at: https://doi.org/10.1081/DRT-120002553.

Iguedjtal, T., Louka, N., & Allaf, K. (2008). Sorption isotherms of potato slices dried and texturized by controlled sudden decompression. *Journal of Food Engineering, 85*(2), 180-190. Available at: https://doi.org/10.1016/j.jfoodeng.2007.06.028.

Kaveh, M., & Amiri Chayjan, R. (2017). Modeling thin-layer drying of turnip slices under semi-industrial continuous band dryer. *Journal of Food Processing and Preservation, 41*(2), e12778. Available at: https://doi.org/10.1111/JFPP.12778.

Key-Technology. (2015). Bulk density averages. Retrieved from http://go.key.net/rs/key/images/Bulk%20Density%20Averages%20100630.pdf.

Larrauri, J. A., Rupérez, P., & Saura-Calixto, F. (1997). Effect of drying temperature on the stability of polyphenols and antioxidant activity of red grape pomace peels. *Journal of Agricultural and Food Chemistry, 45*(4), 1390-1393. Available at: https://doi.org/10.1021/jf960282f.

Lewis, W. K. (1921). The rate of drying of solid materials. *Industrial & Engineering Chemistry, 13*(5), 427-432. Available at: https://doi.org/10.1021/ie50137a021.

Louati, I., Bahloul, N., Besombes, C., Allaf, K., & Kechaou, N. (2019). Instant controlled pressure-drop as texturing pretreatment for intensifying both final drying stage and extraction of phenolic compounds to valorize orange industry by-products (Citrus sinensis L.). *Food and Bioproducts Processing, 114*, 85-94. Available at: https://doi.org/10.1016/J.FBP.2018.11.012.

Louka, N., & Allaf, K. (2004). Expansion ratio and color improvement of dried vegetables texturized by a new process "controlled sudden decompression to the vacuum": application to potatoes, carrots and onions. *Journal of Food Engineering, 65*(2), 233-243. Available at: https://doi.org/10.1016/j.jfoodeng.2004.01.020.

Louka, N., Juhel, F., & Allaf, K. (2004). Quality studies on various types of partially dried vegetables texturized by controlled sudden decompression: General patterns for the variation of the expansion ratio. *Journal of Food Engineering, 65*(2), 245-253. Available at: https://doi.org/10.1016/j.jfoodeng.2004.01.021.

Maache-Rezzoug, Z., Rezzoug, S., & Allaf, K. (2001). Kinetics of drying and hydration of the scleroglucan polymer. A comparative study of two conventional drying methods with a new drying process: dehydration by successive pressure drops. *Drying Technology, 19*(8), 1961-1974. Available at: https://doi.org/10.1081/DRT-100107283.

Maache-Rezzoug, Z., Rezzoug, S., & Allaf, K. (2002). Development of a new drying process–dehydration by cyclical pressure drops (DDS): application to the collagen gel. *Drying Technology, 20*(1), 109-129. Available at: https://doi.org/10.1081/DRT-120001369.

Mounir, S., Besombes, C., Al-Bitar, N., & Allaf, K. (2011). Study of instant controlled pressure drop DIC treatment in manufacturing snack and expanded granule powder of Apple and Onion. *Drying Technology, 29*(3), 331–341. Available at: https://doi.org/10.1080/07373937.2010.491585.

Mounir, S., Téllez-Pérez, C., Alonzo-Macías, M., & Allaf, K. (2014). Swell-drying. In T. Allaf & K. Allaf (Eds.), Instant Controlled Pressure Drop (D.I.C.) in Food Processing (pp. 3–43). New York, NY: Springer.

Obied, H. K., Bedgood Jr, D. R., Prenzler, P. D., & Robards, K. (2008). Effect of processing conditions, prestorage treatment, and storage conditions on the phenol content and antioxidant activity of olive mill waste. *Journal of agricultural and food chemistry, 56*(11), 3925-3932. Available at: https://doi.org/10.1021/jf703756d.

Parra-Coronado, A. (1993). Almacenamiento aireado de maíz en los Llanos Orientales. *Ingeniería e Investigación*(29), 5-13.

Parra-Coronado, A., Roa-Mejía, G., & Oliveros-Tascón, C. E. (2008). SECAFÉ Part I: Modeling and mathematical simulation in the mechanical drying of parchment coffee. *Brazilian Journal of Agricultural and Environmental Engineering, 12*(4), 415-427. Available at: https://doi.org/10.1590/S1415-43662008000400013.

Rakotozafy, H., Louka, N., Therisod, M., Thérisod, H., & Allaf, K. (2000). Drying of baker's yeast by a new method: Dehydration by Successive Pressure Drops (DDS). Effect on cell survival and enzymatic activities. *Drying Technology, 18*(10), 2253-2271. Available at: https://doi.org/10.1080/07373930008917841.

Roa, G., Oliveros, C. E., Álvarez, J., Ramírez, C., Sanz, J. R., Dávila, M. T., & Rodríguez, N. (1999). Coffee drying. In Ecological processing of coffee. Retrived from https://biblioteca.cenicafe.org/handle/10778/882.

Sadeghi, E., Movagharnejad, K., & Haghighi Asl, A. (2019). Mathematical modeling of infrared radiation thin-layer drying of pumpkin samples under natural and forced convection. *Journal of Food Processing and Preservation, 43*(12), e14229. Available at: https://doi.org/10.1111/JFPP.14229.

Shah, Z., Jani, Y. M., & Khan, F. (2014). Evaluation of organic wastes for composting. *Communications in Soil Science and Plant Analysis, 45*(3), 309-320. Available at: https://doi.org/10.1080/00103624.2013.861909.

Sotiropoulos, A., Malamis, D., Michailidis, P., Krokida, M., & Loizidou, M. (2016). Research on the drying kinetics of household food waste for the development and optimization of domestic waste drying technique. *Environmental Technology, 37*(8), 929-939. Available at: https://doi.org/10.1080/21622515.2015.1092588.

Thompson, T., Peart, R., & Foster, G. (1968). Matllematical simulation of corn drying a new model. *Transaction of the ASAE, 11*(4), 582-586. Available at: https://doi.org/10.13031/2013.39473.

Wang, C. Y., & Singh, R. (1978). Single layer drying equation for rough rice. *Transactions of the ASAE*.

Wuttipalakorn, P., Srichumpuang, W., & Chiewchan, N. (2009). Effects of pretreatment and drying on composition and bitterness of high-dietary-fiber powder from lime residues. *Drying Technology, 27*(1), 133-142. Available at: https://doi.org/10.1080/07373930802566036.

Yagcioglu, A. K., Degirmencioglu, A., & Cagatay, F. (1999). *Drying characteristics of laurel leaves under different drying conditions.* Paper presented at the 7th Int Congress Agricultural Mechanisation and Energy, May 1999, 565–569.

Yaldız, O. (2001). Thin layer solar drying of some vegetables. *Drying Technology, 19*(3–4), 583-597. Available at: https://doi.org/10.1081/DRT-100103936.